Acta Ophthalmologica

Acta Ophthalmologica 2020

Analysis of the location of retinal lesions in central retinographies of patients with Type 2 diabetes

Eduardo Munuera-Gifre,[1] Marc Saez,[1,2,3] Dolors Juvinyà-Canals,[4] Antonio Rodríguez-Poncelas,[1] Joan-Francesc Barrot-de-la–Puente,[5] Josep Franch-Nadal,[5] Pere Romero-Aroca,[6] Maria Antonia Barceló[1,2,3] and Gabriel Coll-de-Tuero[1,3,7]

[1]METHARISC Group, USR Girona, IdIAP Gol i Gorina, Girona, Spain
[2]Research Group on Statistics, Econometrics and Health (GRECS), University of Girona, Girona, Spain
[3]CIBER of Epidemiology and Public Health (CIBERESP), Madrid, Spain
[4]Faculty of Nursing, University of Girona, Girona, Spain
[5]USR Barcelona, IdIAP Gol i Gorina, Barcelona, Spain
[6]Ophthalmology Service, University Hospital Sant Joan, Institut d'Investigació Sanitària Pere Virgili (IISPV), University Rovira i Virgili, Reus, Spain
[7]Department of Medical Sciences, University of Girona, Girona, Spain

ABSTRACT.

Purpose: **To describe the distribution of Type 2 DM retinal lesions and determine whether it is symmetrical between the two eyes, is random or follows a certain pattern.**

Methods: **Cross-sectional study of Type 2 DM patients who had been referred for an outpatients' ophthalmology visit for diabetic retinopathy screening in primary health care. Retinal photographic images were taken using central projection non-mydriatic retinography. The lesions under study were microaneurysms/haemorrhages, and hard and soft exudates. The lesions were placed numerically along the x- and y-axes obtained, with the fovea as the origin.**

Results: **From among the 94 patients included in the study, 4770 lesions were identified. The retinal lesions were not distributed randomly, but rather followed a determined pattern. The left eye exhibited more microaneurysms/haemorrhages and hard exudates of a greater density in the central retina than was found in the right eye. Furthermore, more cells containing lesions were found in the upper temporal quadrants, (especially in the left eye), and tended to be more central in the left eye than in the right, while the hard exudates were more central than the microaneurysms/haemorrhages.**

Conclusion: **The distribution of DR lesions is neither homogeneous nor random but rather follows a determined pattern for both microaneurysms/haemorrhages and hard exudates. This distribution means that the areas of the retina most vulnerable to metabolic alteration can be identified. The results may be useful for automated DR detection algorithms and for determining the underlying vascular and non-vascular physiopathological mechanisms that can explain these differences.**

Key words: diabetic retinopathy – exudates – haemorrhages – microaneurysms – type 2 DM retinal lesions

Acta Ophthalmol. 2020: 98: e13–e21

doi: 10.1111/aos.14223

Introduction

Worldwide Type 2 diabetes mellitus (DM) is a highly prevalent illness and exhibits an increasing tendency for the near future (Zimmet et al. 2014). Diabetic retinopathy (DR) is a common complication in Type 2 DM and is the number one cause of blindness worldwide (Lee et al. 2015). Likewise, mild forms of DR are associated with cardiovascular (CV) and kidney disease risk (Liew et al. 2009; Mottl et al. 2012; Penno et al. 2012).

Metabolic controls and controls for other risk factors such as hypertension, reduce the risk of macro- and microvascular complications, such as DR, in Type 2 DM (Gaede et al. 2003). Early detection of DR is important so that suitable medication can be administered to stop its progression to serious forms of retinopathy and to avoid blindness. Microaneurysms are the target lesions in diabetic retinopathy (ETDRS Report number 12, 1991). The purpose of DR screening is the early detection of microaneurysms and haemorrhages. Thus, developing automated methods that can detect and classify typical DR lesions and that can analyse a large number of retinographic images in a short period of time is extremely interesting as this would mean DR screening could be

carried out with a very few resources. Currently, the most commonly used methods are based on improving lesion identification (Sánchez et al. 2008, 2009; Sopharak et al. 2013; Navarro et al. 2016; Srivastava et al. 2017), classifying them based on class imbalance (Dai et al. 2016; Wu et al. 2017) and, more recently, applying deep convolutional neural network (CNN) technology (Ordóñez et al. 2017; Xu et al. 2017).

The distribution of lesions typical in Type 2 DM has been reported as not being uniform in either animal or human models, and the likelihood of lesions appearing has been observed to vary depending on the area in the retina (Kern & Engerman 1995; Tang et al. 2003; Silva et al. 2007, 2015). A detailed description of these lesions could be enormously helpful in formulating hypotheses about the physiopathological mechanisms of DR and to optimize the readings of the images obtained by both manual and automated retinography.

Patients and methods

Patients

Patients with Type 2 DM who had been referred for diabetic retinopathy screening in primary health care and who met the inclusion criteria were consecutively included. The patients were examined during an ophthalmology outpatient clinic visit. The inclusion criteria were as follows: a clear and interpretable retinography, well-centred central retinographies for both eyes, and no other type of lesion in the retina that could be confused with diabetic lesions such as photocoagulation and photographic artefacts. The presence of retinal alterations that could give a margin of error (e.g. chorioretinitis, artefact images, myelinated fibres) was also a reason for exclusion. All the patients were informed about the study and gave their consent. Approval for the study was obtained from the Institutional Review Board (IRB), and the research described here adhered to the tenets of the Declaration of Helsinki.

Methods

The retinographies were centred on the macular area using a non-mydriatic retinal camera (TOPCON TRC-NW6S, Topcon Medical Systems, Tokyo, Japan) at 45°, thus allowing the entire central retina and the posterior crown of the peripheral retina to be visualized. The images were placed in the same position on the screen of an HP 1523 monitor with a 1024 × 768 resolution (Hewlett-Packard, Palo-Alto, USA) PC. The images were analysed to the maximum size allowed by the screen, that is 55%. If necessary, the zoom in the Microsoft Windows 8 Paint programme (Redmond, Washington, USA) was used to enlarge the image screen. The lesions under study were recorded and placed numerically using the x- and y-axes obtained with the fovea as the origin (Fig. 1). In the case of hard exudates and microaneurysms, since they are very small, they are always placed in a single cell. A few microhaemorrhagic lesions may affect more than one cell; in this case, they were assigned to the cell that contained the centre of the lesion. In the case of soft exudates, only their location in crowns was considered. The geometric centre corresponds to the fovea.

The retina examination was divided into two procedures. First, a tangential, internal circumference was outlined on the surface of the optic disc with the fovea at its centre. This delimited surface area was considered as the central retina. A tangential circumference external to the optic disc was added concentrically to the first, along with two others with radiuses of 2/3 and 1/3 with respect to the radius of the circumference delimiting the central retina (Figure S1).

Fig. 1. Location of lesions by 'x' and 'y' axis. *x*-axis: 214 px. *y*-axis: 174 px. Cell n° 17. Crown b.

Second, the retinal surface area was divided into squares. For this, a virtual grid divided into squares of 54.857 side pixels (of screen) was superimposed on the central retinograph. Each cell had coordinates defined on both axes. The lesions were located in a determined cell according to the coordinates. The square cells were numbered symmetrically from 1 to 41. The shaft axes of the square that made up the grid with the fovea as its centre were accepted as cartesian axes. Figure 2 shows the relationship of the cells with the central circle and crowns.

Validation of the observer

One of the authors (EMG), who is an ophthalmologist and pathologist, checked all the retinographies to identify the lesions. The images were anonymized. The reading order for the intraobserver agreement was random and differed between the first and second reading. Interobserver agreement was assessed by another expert (JBP) as well as with the intraobserver. The results obtained from the interobserver and intraobserver agreement for the soft and hard exudates and the microaneurysms/haemorrhages in a sample of 50 images shows a kappa correlation coefficient of >0.9.

External validation of the sample

In a universal healthcare system, a selection bias summary reduces but does not totally eliminate this prospect, so the external validity of the sample was checked by comparing the characteristics of the patients with other

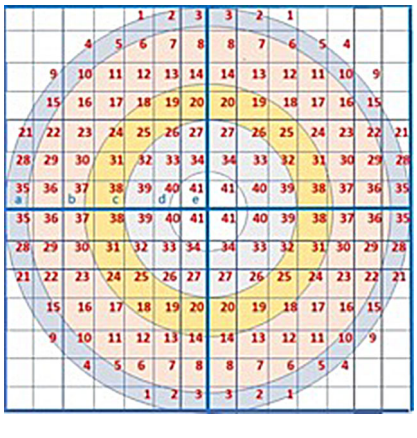

Fig. 2. Relationship of the cells with the central circle and crowns.

primary healthcare cohorts from the same region (see Results).

Identifying and locating lesions

Three types of lesions were identified and located: microaneurysms/haemorrhages, and hard and soft exudates. When each lesion was identified, its coordinates (in pixels) were determined and a hemiretina, quadrant, crown, central circle and cell assigned to it.

Retinal areas occupied by lesions

The density (number of lesions per 100 pixeles^2 for microaneurysms, haemorrhages and hard exudates and number of lesions per 1000 pixeles^2 for soft exudates) of each type of lesion was calculated from the hemiretina, quadrants and crowns. Cell occupation by lesions was expressed through two variables. First, the cells in each quadrant were ordered by the number of each type of lesion they contained and expressed as the five cells in each quadrant containing the most lesions of each type. Second, the cells occupied by each type of lesion were identified, using the maximum value of the cell in the quadrant with the fewest lesions in the retinography of the two eyes separately as the cut-off point. This procedure was used to identify the cells most prone to presenting lesions across the set of four quadrants.

Statistical analysis

The results were expressed as percentages for the categorical variables and as means (SD) and medians (IQR) for the quantitative variables. The Kolmogorov test was applied to determine the distribution of the variables. To compare the qualitative and quantitative variables, a t-test was used if the distribution was symmetrical and a Wilcoxon test if the distribution was non-symmetrical, with a Bonferroni correction in both cases. Using a regular grid spatial design, a logistic regression model was specified to contrast the null hypothesis that the cells defining the 'white hole' (the area of the eye with no lesions) observed in the eyes of all the individuals were distinct to each of them. In other words, the 'white hole' appears randomly. The responding variable was dichotomous, taking the value 1 for cells 12, 13, 14, 18, 19, 20, 26, 27 and 34 in quadrants III (right eye) and VI (left eye), and the value 0 for the rest of the cells. Two random effects were introduced into the model, one which collected individual heterogeneity (i.e. the non-observed factors specific to each cell that could explain the presence of lesions in it), and another that collected the spatial dependency between cells (i.e. the likelihood that the occurrence of a lesion in a cell could increase the probability of a lesion occurring in neighbouring cells).

It was assumed that the random effect that collected heterogeneity was distributed normally, identically and independently. For the random effect collected by the spatial dependence, a Matérn structure was considered suitable (Lindgren et al. 2011).

This model was used to test the null hypothesis that there is no difference between quadrants III (right eye) and VI (left eye). Using the same grid design, a Poisson regression model was then described to contrast the null hypothesis that the lesions were distributed homogeneously among all the cells and/or areas of the eye. In this case, the response variable was the number of lesions in each cell. As in the logistic regression, a random effect to collect individual heterogeneity and other spatial dependence was introduced.

Results

The sample size comprised 94 patients with Type 2 DM (51% women), and the mean age was 64.8 years (SD8.6). Table 1 shows the other characteristics.

This sample was compared with data from the two large cohorts in our region. The first cohort (Rodriguez-Poncelas et al. 2015) made up of 108,723 patients with Type2DM from all over Catalonia, Spain referred for a DR early detection retinography, showed no differences regarding sex, HbA1c or prevalence of hypertension. This cohort was slightly younger (64.8 versus 66.9 years; $p = 0.02$) and received less insulin treatment. The other benchmark cohort (Romero-Aroca et al. 2016) was from Tarragona, Catalonia, Spain and comprised 15 396 Type 2 DM patients who had also been referred for a DR early detection retinography. This cohort showed no differences in age, sex, HbA1c, prevalence of hypertension and treatment with insulin with respect to the cohort in this study.

From the retinographies taken, 4770 lesions were identified and located of which 2785 were in the central retina, 1302 of these were in the right eye and 1483 were in the left eye. Hard exudates were more common than microaneurysms/haemorrhages in the central retinas, and both types of lesions were more frequent in the left central retina. There was a greater density of microaneurysms/haemorrhages and hard exudates in the central retina of the left eye (0.38 versus 0.32 lesions/100 pixels^2; $p < 0.001$). Furthermore, there was a greater density of all lesion types in the central retina than in the peripheral retina of both eyes (Table S1).

There was a greater density of hard exudates in the upper, rather than in the lower, hemiretinas of both eyes. However, this difference was not observed for microaneurysms/haemorrhages or soft exudates. On comparing the densities of the lesions in the upper hemiretinas of both central retinas, all were shown to have a greater density in the upper left, rather than the upper right, hemiretina. (Table S2).

There were greater densities of microaneurysms/haemorrhages in the temporal hemiretinas of both eyes than in the nasal hemiretinas, and in the left temporal hemiretina rather than in the right. There was also a greater density of soft exudates in the left temporal hemiretina than in the nasal hemiretina on the same side, with no observable

Table 1. Characteristics of participants with Type 2 diabetes (n = 94).

Gender, women, n (%)	49 (51)
Age, years (SD)	64.8 (8.6)
Visual acuity (SD)	
Right eye	0.80 (0.22)
Left eye	0.79 (0.19)
Intraocular pressure, mmHg (SD)	
Right eye	17 (3.4)
Left eye	17 (3.6)
Hypertension, n, (%)	74 (79)
HbA1c, % (SD)	7.4 (1.7)
Dislipemia, n ((%)	89 (94.3)
Antihypertensive treatment, n (%)	61 (65)
ACEI/ARB treatment, n (%)	51 (54.2)
Hipolipemiant treatment, n (%)	65 (69.1)
Antidiabetic treatment, n (%)	87 92.5)
Insulin treatment, n (%)	31 (33)

differences between the two hemiretinas in the right eye.

There was a greater density of microaneurysms/haemorrhages and hard exudates in the central retina (c, d, circular crowns) of both eyes, and these lesions were more concentric (d circular crown) and denser in the left eye, especially in the case of the hard exudates. The soft exudates were denser and more concentric in the circular crowns of the right eye (Table S3).

Figure 3 shows the five cells in each quadrant with the most microaneurysms/haemorrhages and hard exudates. It can be seen that, when considering all the quadrants simultaneously and with a cut-off point corresponding to the number of lesions in the most occupied cell in the quadrant with the fewest lesions (Fig. 4), all the cells with the most microaneurysms/haemorrhages and hard exudates coincide with the cells that present the most lesions in each quadrant analysed separately. Figure 5 is a three-dimensional representation of the total number of lesions in each cell. As before, it can be seen that there are more lesions of all types (subject to this study) in the temporal hemiretinas and the upper hemiretinas, so it is in the upper temporal quadrant, especially of the left eye, where the cells that are occupied by the most lesions are found.

Given the results from the adjusted logistic regression model, which show

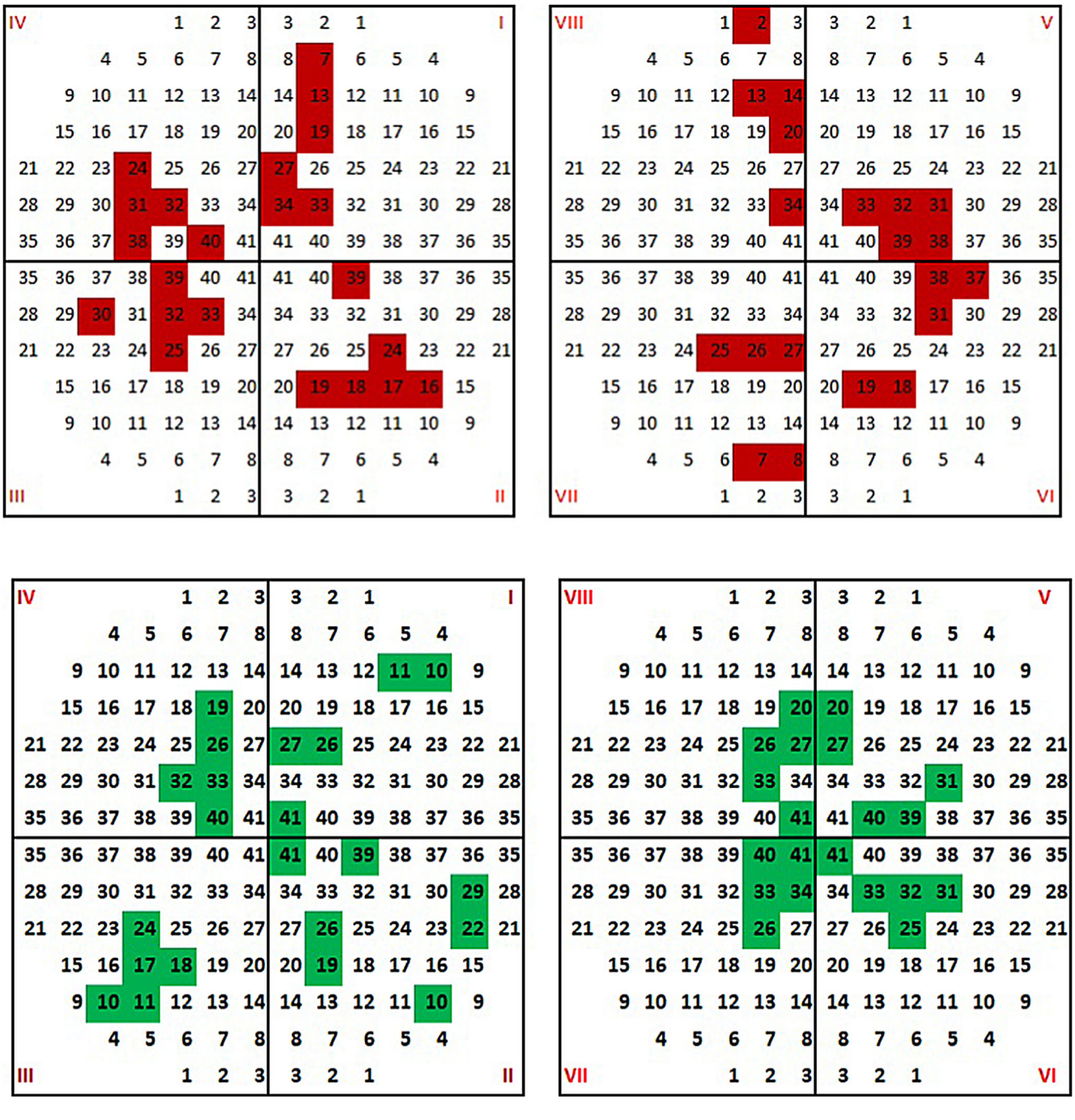

Fig. 3. Five cells in each quadrant with the highest number of retinopathy lesions: microaneurysms/haemorrhages (red) and hard exudates (green).

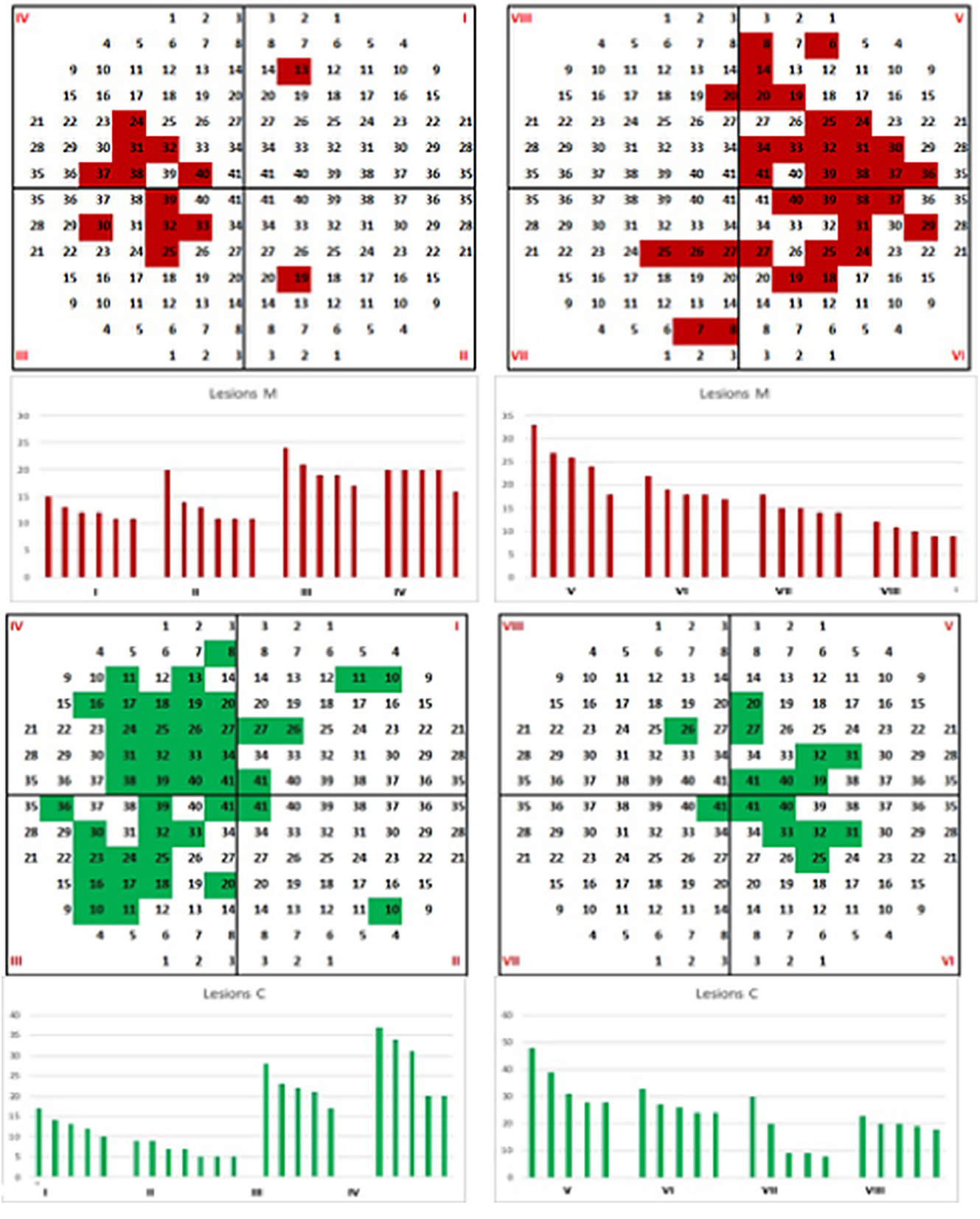

Fig. 4. Cells with the greatest presence of microaneurysm/haemorrhages (red) and hard exudates (green) in all quadrants. Figure 2 shows the cells in each quadrant occupied by microaneurysms/microbleeds and hard exudates using the maximum value of the quadrant cell with the lowest number of lesions as the cut-off point.

that the distribution of the lesions and the area without lesions are not random, the null hypothesis that the lesion-free oval area is down to chance can be rejected. The cells with more lesions than expected are shown in Fig. 6. The highest number of cells occupied with more DR lesions than expected, can be seen to be in the upper

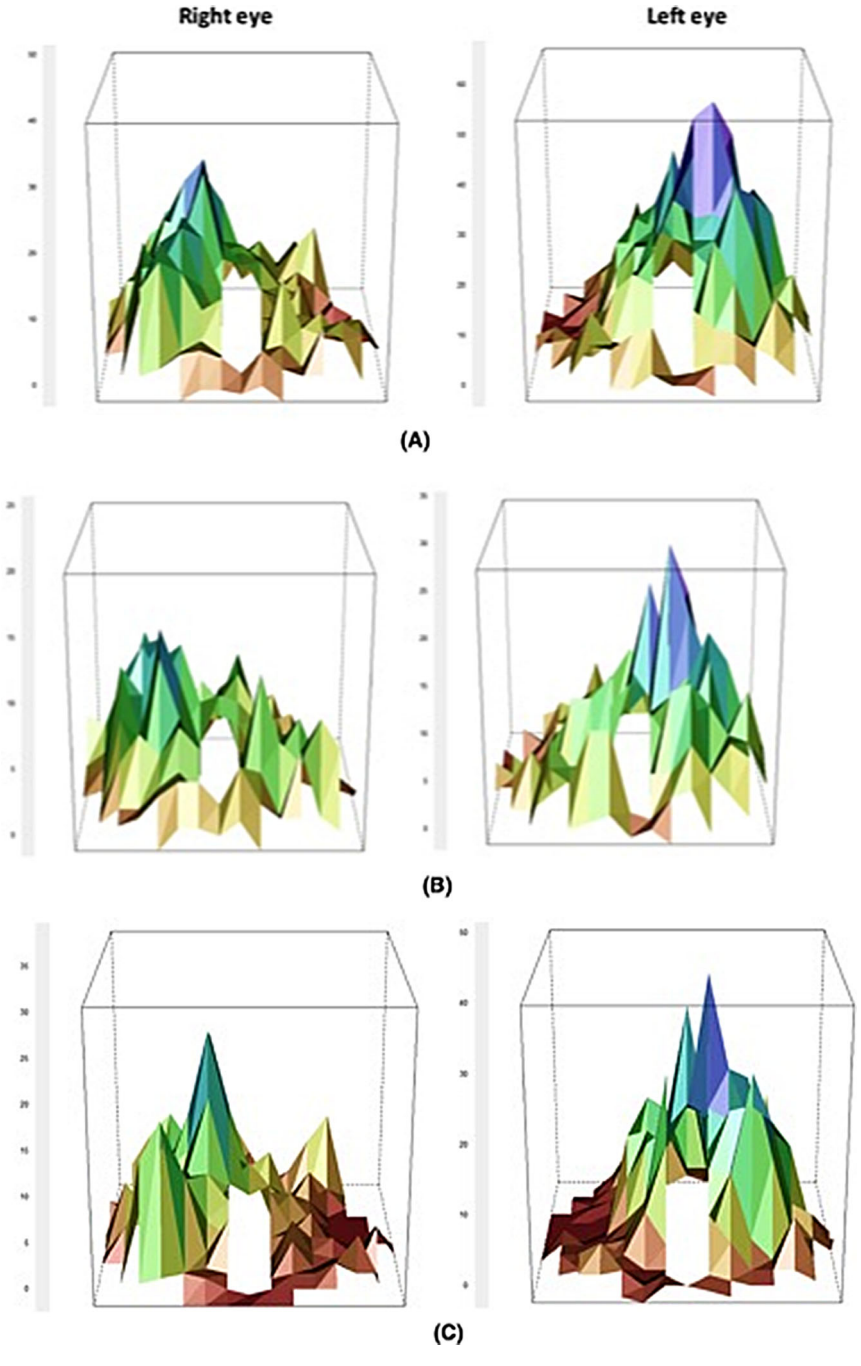

Fig. 5. Distribution of lesions in the retinography of both eyes. (A) All lesions. (B) Microaneurysms/haemorrhages. (C) Hard exudates. The figures show the distribution of the lesions in the central retina quadrants. The results show that the distribution of lesions and lesion-free zone (white hole) are not random ($p < 0.005$). In the model, two random effects were introduced, one that included individual heterogeneity, that is those factors specific to each cell, not observed that could explain the existence of lesions in the cell; another that collected the (spatial) dependence between cells, that is the occurrence of an injury in a cell could increase the probability of the occurrence of an injury in the neighbouring cells.

temporal quadrants of both eyes, in particular in the left eye. These results have been obtained using an adjusted Poisson regression model and are expressed in percentages of occupation of each cell above the expected percentages. The cells most expected to be occupied that coincide with the highest absolute number of lesions are numbers 30, 31, 36 and 37 in the upper temporal quadrant (V) and cells 37 and 38 in the lower temporal quadrant (III) of the left eye. In the right eye, cells 24, 37 and 38 in the upper temporal quadrant and cell 30 in the lower temporal quadrant are the ones most expected to be occupied. (See Annex S1).

Discussion

Our results show that central retina lesions in patients with Type 2 DM are not distributed randomly but rather follow a fixed pattern. There are more microaneurysms/haemorrhages and hard exudates in the left eye than in the right. When the density of the lesions is analysed using 100 pixeles^2, the density of the microaneurysms/haemorrhages and hard exudates is observed as being greater in the left central retina than in the right (0.38 versus 0.32 lesions/100 pixeles^2; $p < 0.001$). The lesions are located, to a significant extent, in the temporal and upper hemiretinas, with the upper temporal quadrants containing the most cells occupied by lesions, especially in the left eye. Furthermore, the lesions tend to be more central in the left eye than in the right and the hard exudates tend to be more central than the microaneurysms/haemorrhages. The lesion-free oval area, which appears in the central retinas of both eyes, could be related to embryonic fissure when the retina is forming.

It was presumed that the cells with the most lesions are those with a more active histology in their formation, that is the ones most vulnerable to the metabolic disorder Type 2 DM. Thus, it can be concluded that histological components that respond differently to this metabolic alteration are involved in the two types of lesions. As expected, the set of microaneurysms/haemorrhages follows a predominantly vascular configuration, which is illustrated by the macroscopic aspect, regularity in the distribution and scarcity in the perifoveal area. The set of information obtained from the behaviour of the microaneurysms/haemorrhages as a whole, however, allows us to go beyond simply adjudicating this to the vascular component to interpret more subtle aspects of the configuration and behaviour of this retinal vascular network that would be difficult to obtain by observation under a microscope. For example, the difference in densities between both central retinas, the difference between the nasal and temporal hemiretinas, the differences between

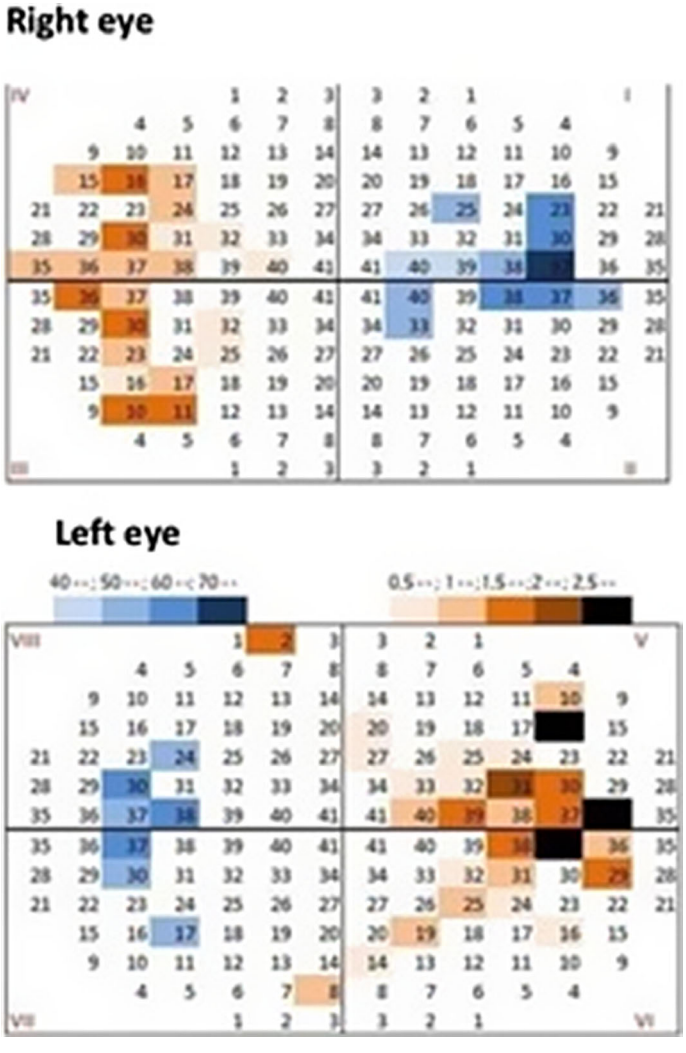

Fig. 6. Cells in each quadrant with significantly more (brown) or fewer (blue) lesions than expected (in percentage). Poisson regression model to contrast the null hypothesis that the lesions were distributed homogeneously among all the cells and/or areas of the eye. The response variable was the number of lesions in each cell. Logistic regression, a random effect to collect individual heterogeneity and another spatial dependence (See Annex S1).

the crowns in the right and left central retinas and the different distribution of cells with most lesions, all point to there being inequalities in the distribution of blood vessels and differences in both their physiological functions and their response to this metabolic aggression and other risk factors, both between the two retinas and within each of them. In this sense, a recent article (Ometto et al. 2017) shows that the microaneurysms/microhaemorrhages located in the first perimacular circle predict the progression of retinal lesions. Our study shows that microaneurysms/microhaemorrhages appear earlier in the temporal cells adjacent to the macula (located in the first perimacular crown) and suggest that these cells are the most active in the formation of these lesions. The distribution of hard exudates follows a pattern that does not correspond to any specific histological structure, suggesting that the histological component of the retina involved in its formation also varies depending on the area. These histological differences are currently outside the scope of mere microscopic observation. Given that the retina belongs to the central nervous system, these variations in histological composition would be reflected in subtle differences between the different regions of the neural component of the central nervous system involved in vision. The early stages of DR are accompanied by dilatation of the diameter of the retinal vessels and reduced autoregulation, demonstrating that there are differences in the different areas of the retina (Bek 2017). In this regard, regional differences in the diameter response to increased blood pressure have been described, which could partially explain the differences in the formation and distribution of lesions (Skov Jensen et al. 2011). A study that measured overall oxygen saturation found that this decreased from the upper and lower nasal quadrant and from the lower temporal quadrant to the upper temporal quadrant, which corresponds to the area where there are most lesions, although this decrease in O_2 saturation was found in healthy patients as well as in those with Type 2 DM or DR (Jørgensen & Bek 2017). A recent study based on an animal model of diabetic mice showed that low regulation of the expression of connexin 43 induced cell death and increased the permeability of the vessels in the retina, which acted as a promotor mechanism of RD (Tien et al. 2014). The prior work of Tang et al. (2003) showed that while there are more microaneurysms in the temporal hemiretina, no differences were found in the thickness of the retinal capillary basement membrane across the retina. The only difference they found between quadrants was in the activity of a protease, caspase 1. They also found a greater expression of nitric oxide synthase (iNOS) in the temporal hemiretina of patients with Type 2 DM. iNOS is involved in vascular tone, angiogenesis and neural development. These data point to DR lesions not only responding to a vascular mechanism, but to their having a neurodegenerative component of the associated retina. In other words, it seems that DR is the expression of the vulnerability of certain areas of the retina to various vascular risk factors that act on the level of the vascular and metabolic autoregulation (iNOS, vessel calibre, connexin 14) of the entire retina.

There is a low density of lesions in the area we have called the 'external retina' (ER), but there are no apparent distribution patterns, leading us to believe that it is at the 'central retina' (CR) level where the distribution of the tissues involved in the appearance of diabetic lesions is well-organized and that the rest of the retina studied in this article (the ER) does not share the same organizational characteristics.

The results of our study not only show the differences in the distribution of lesions in the retina and the densities with histological and physiopathological implications for future studies, but they can also assist technological transfer in detecting retina lesions typical of DR. In recent years, convolutional neural networks (CNNs) have been shown to be a deep-learning method that gives excellent results in terms of sensitivity, specificity, agreement and precision in detecting RD in general (Gulshan et al. 2016; Gargeya & Leng 2017; Ting et al. 2017; Krause et al. 2018) and microaneurysms and haemorrhages in particular (Chudzik et al. 2018). However, CNNs have several limitations that affect their practical application. First, lesions in the initial stages of RD are scarce and are found in less than 1% of the total number of pixels, which hinders their detection. Furthermore, deep learning requires larger image datasets for training and, finally, the time needed to analyse the retina is about one minute, which is quite long for a screening technique (Lam et al. 2018). Our results can be useful for alerting expert systems about which cells must be checked and in which order when searching for lesions typical of DR, thus reducing the false-negative margins; in other words, increasing the sensitivity of the algorithms. Reducing the size of the retinal area to explore would probably decrease the time needed to analyse each image. However, further studies are required to assess these possibilities.

Among the strengths of this study are the high number of DR lesions analysed, the use of a solid methodology and readings by a single observer who is an expert in retinal diseases and a high inter- and intraobserver agreement with another expert involved in this study. This high agreement has been previously described for patients with hypertension (Enström et al. 2000). This study has limitations that should be considered. Not knowing the laterality of the patient, that is if they are right- or left-handed. The predominance of determinate lesions in one eye and in the adelphus could be related to stereoscopic vision, which may induce physiopathological changes of varying intensity in different areas of the retina. The limitations in our study include that the severity scale could vary if we use wide-field image techniques such as Optovue, and the number of patients with advanced DR can increase by 12%, despite the nine retinographies being able to achieve retinal periphery (Silva et al., 2007, 2015). However, the objective of this work was to determine the distribution of lesions in the central retina by using standard retinography as it is still the most accessible DR screening technique. Although not an objective of our study, peripheral retinal lesions were assessed for clinical effects.

In conclusion, the main finding of our study is that the distribution of DR lesions is neither homogeneous nor random but follows a determined pattern for microaneurysms/haemorrhages and hard exudates. This distribution, (based on the sequence of appearance of the lesions and the expectation of the cells being occupied), means we can identify the areas of the retina that are most vulnerable to metabolic alteration. The results could contribute to opening new lines of research to determine the vascular physiopathological mechanisms that explain these differences. Moreover, the results may be useful for the automated DR detection algorithms, facilitating deep learning and shortening retinal image analysis time.

Authors contributions

EM and GCT had the original idea of the paper and designed the study. The bibliographical search and the writing of the introduction were made by EM, GCT and ARP. The choice of methods and statistical analyses was performed by GCT, MAB and MS. EM, GCT and MS built the tables and figures. EM, GCT, ARP, JFB, JFN and PRA wrote the results and the discussion. The writing and final editing were done by all the authors. All authors reviewed and approved the manuscript.

Data availability

Due to the restrictions on the transfer of data to third parties, both ethical (accordance of the protocol approved by the Ethics and Clinical Research Committee of the Institute of Health Care (IAS), Girona, Spain) and legal (according to the provisions of the Spanish Law on Data Protection, Fundamental Law 15/1999 of 13 December on the Protection of Personal Data, article 7.3); data (appropriately anonymized) will be available to all interested researchers upon request to Gabriel Coll-de-Tuero (gcolld@comg.cat).

References

Bek T (2017): Diameter changes of retinal vessels in diabetic retinopathy. Curr Diab Rep **17**: 82.

Chudzik P, Majumdar S, Calivá F, Al-Diri B & Hunter A (2018): Microaneurysm detection using fully convolutional neural networks. Comput Methods Programs Biomed **158**: 185–192.

Dai B, Wu X & Bu W (2016): Retinal microaneurysms detection using gradient vector analysis and class imbalance classification. PLoS ONE **11**: e0161556.

Enström I, Burtscher IM, Eskilsson J, Holm K, Holtàs S, Pennert K & Thulin T (2000): Organ damage in treated middle-aged hypertensives compared to normotensives: results from a cross-sectional study in general practice. Blood Press **9**: 28–33.

ETDRS Report number 12. Early Treatment Diabetic Retinopathy Study Research Group Ophthalmology. (1991): Fundus photographic risk factors for progression of diabetic retinopathy. Ophthalmology **98** (5 Suppl): 823–833.

Gaede P, Vedel P, Larsen N, Jensen GV, Parving HH & Pedersen O (2003): Multifactorial intervention and cardiovascular disease in patients with type 2 diabetes. N Engl J Med **348**: 383–393.

Gargeya R & Leng T (2017): Automated identification of diabetic retinopathy using deep learning. Ophthalmology **124**: 962–969.

Gulshan V, Peng L, Coram M et al. (2016): Development and validation of a deep learning algorithm for detection of diabetic retinopathy in retinal fundus photographs. JAMA **316**: 2402–2410.

Jørgensen CM & Bek T (2017): Lack of differences in the regional variation of oxygen saturation in larger retinal vessels in diabetic maculopathy and proliferative diabetic retinopathy. Br J Ophthalmol **101**: 752–757.

Kern TS & Engerman RL (1995): Vascular lesions in diabetes are distributed non-uniformly within the retina. Exp Eye Res **60**: 545–549.

Krause J, Gulshan V, Rahimy E, Karth P, Widner K, Corrado GS, Peng L & Webster DR (2018): Grader variability and the importance of reference standards for evaluating machine learning models for diabetic retinopathy. Ophthalmology **125**: 1264–1272.

Lam C, Yu C, Huang L & Rubin D (2018): Retinal lesion detection with deep learning using image patches. Invest Ophthalmol Vis Sci **59**: 590–596.

Lee R, Wong TY & Sabanayagam CH (2015): Epidemiology of diabetic retinopathy, diabetic macular edema and related vision loss. Eye Vis (Lond) **2**: 17.

Liew G, Wong TY, Mitchell P, Cheung N & Wang JJ (2009): Retinopathy predicts coronary heart disease mortality. Heart **95**: 391–394.

Lindgren F, Rue H & Lindström J (2011): An explicit link between Gaussian fields and Gaussian Markov random fields: the stochastic partial differential equation approach (with discussion). J R Stat Soc Series B **73**: 423–498. [Available at: https://www.math.ntnu.no/inla/r-inla.org/papers/spde-jrssb-revised.pdf, last accessed on October 27, 2018].

Mottl AK, Kwon KS, Garg S, Mayer-Davis EJ, Klein R & Kshirsagar AV (2012): The association of retinopathy and low GFR in type 2 diabetes. Diabetes Res Clin Pract **98**: 487–493.

Navarro PJ, Alonso D & Stathis K (2016): Automatic detection of microaneurysms in diabetic retinopathy fundus images using the L*a*b color space. Opt Soc Am A Opt Image Sci Vis **33**: 74–83.

Ometto G, Assheton P, Calivá F, Chudzik P, Al-diri B, Hunter A & Bek T (2017): Spatial distribution of early red lesions is a risk factor for development of vision-threatening diabetic retinopathy. Diabetologia, **60**: 2361–2367.

Ordóñez PF, Cepeda CM, Garrido J & Chakravarty S (2017): Classification of images based on small local features: a case applied to microaneurysms in fundus retina images. J Med Imaging (Bellingham) **4**: 041309.

Penno G, Solini A, Zoppini G et al. & Renal Insuficiency And Cardiovascular Events (RIACE) Study Group (2012): Rate and determinants of association between advanced retinopathy and chronic kidney disease in patients with type 2 diabetes: the renal insufficiency and cardiovascular events (RIACE) Italian multicenter study. Diabetes Care **35**: 2317–2323.

Rodriguez-Poncelas A, Miravet-Jiménez S, Casellas A, Barrot-De La Puente JF, Franch-Nadal J, López-Simarro F, Mata-Cases M & Mundet-Tudurí X (2015): Prevalence of diabetic retinopathy in individuals with type 2 diabetes who had recorded diabetic retinopathy from retinal photographs in Catalonia (Spain). Br J Ophthalmol **99**: 1–6.

Romero-Aroca P, de la Riva-Fernandez S, Valls-Mateu A, Sagarra-Alamo R, Moreno-Ribas A, Soler N & Puig D (2016): Cost of diabetic retinopathy and macular oedema in a population, an eight year follow up. BMC Ophthalmol **16**: 136.

Sánchez CI, Hornero R, López MI, Aboy M, Poza J & Abásolo D (2008): A novel automatic image processing algorithm for detection of hard exudates based on retinal image analysis. Med Eng Phys **30**: 350–357.

Sánchez CI, García M, Mayo A, López MI & Hornero R (2009): Retinal image analysis based on mixture models to detect hard exudates. Med Image Anal **13**: 650–658.

Silva PS, El-Rami H, Barham R et al. (2007): Hemorrhage and/or Microaneurysm Severity and Count in Ultrawide Field Images and Early Treatment Diabetic Retinopathy Study Photography. Ophthalmology **124**: 970–976.

Silva PS, Cavallerano JD, Haddad NM et al. (2015): Peripheral lesions identified on ultrawide field imaging predict increased risk of diabetic retinopathy progression over 4 years. Ophthalmology **122**: 949–956.

Skov Jensen P, Jeppesen P & Bek T (2011): Differential diameter responses in macular and peripheral retinal arterioles may contribute to the regional distribution of diabetic retinopathy lesions. Graefes Arch Clin Exp Ophthalmol **249**: 407–412.

Sopharak A, Uyyanonvara B & Barman S (2013): Simple hybrid method for fine microaneurysm detection from non-dilated diabetic retinopathy retinal images. Comput Med Imaging Graph **37**: 394–402.

Srivastava R, Duan L, Wong DWK, Liu J & Wong TY (2017): Detecting retinal microaneurysms and hemorrhages with robustness to the presence of blood vessels. Comput Methods Programs Biomed **138**: 83–91.

Tang J, Mohr S, Du YD & Kern TS (2003): Non-uniform distribution of lesions and biochemical abnormalities within the retina of diabetic humans. Curr Eye Res **27**: 7–13.

Tien T, Muto T, Barrette K, Challyandra L & Roy S (2014): Downregulation of Connexin 43 promotes vascular cell loss and excess permeability associated with the development of vascular lesions in the diabetic retina. Molecular Vision **20**: 732–741.

Ting DSW, Cheung CY, Lim G et al. (2017): Development and validation of a deep learning system for diabetic retinopathy and related eye diseases using retinal images from multi-ethnic populations with diabetes. JAMA **318**: 2211–2223.

Wu B, Zhu W, Shi F, Zhu S & Chen X (2017): Automatic detection of microaneurysms in retinal fundus images. Comput Med Imaging Graph **55**: 106–112.

Xu K, Feng D & Mi H (2017): Deep convolutional neural network-based early automated detection of diabetic retinopathy using fundus image. Molecules **22**. pii: E2054. https://doi.org/10.3390/molecules22122054.

Zimmet PZ, Magliano DJ, Herman WH & Shaw JE (2014): Diabetes: a 21st century challenge. Lancet Diab Endocrinol **2**: 56–64.

Received on October 27th, 2018.
Accepted on July 25th, 2019.

Correspondence:
Marc Saez, PhD, CStat, CSci
Research Group on Statistics
Econometrics and Health (GRECS)
CIBER of Epidemiology and Public Health (CIBERESP)
University of Girona
Carrer de la Universitat de Girona 10
Campus de Montilivi
17003 Girona
Spain
Tel: 34-972-418338
Fax: 34-972-418032
Email: marc.saez@udg.edu; http://www.udg.edu/grecs.htm

We appreciate the comments of one anonymous reviewer of a previous version of this work who, without doubt, helped us to improve our work.

The manuscript is an original contribution that has not been published before, whole or in part, in any format, included electronically. All authors will disclose any actual or potential conflict of interest including any financial, personal or other relationships with other people or organizations that could inappropriately influence or be perceived to influence their work, within three years of beginning the submitted work.

This work was partly funded by the research project PI15/00140 from FIS, 'Instituto de Salud Carlos III', ISCIII, Spanish Ministry of Economy and Competitiveness and by the projects MPCUdG2016 and GDRCompetUdG2017 of the University of Girona. The funders had no role in study design, data collection and analysis, decision to publish, or preparation of the manuscript.

Supporting Information

Additional Supporting Information may be found in the online version of this article:

Figure S1. Central circle, circular crowns and cells.
Table S1. Amount and density of diabetic retinopathylesions. N = 4770
Table S2. Densities of diabetic retinopathy lesions according to hemiretins of the same eye and both eyes.
Table S3. Density of lesions according to circular crowns.
Annex S1. Cells with lower lessions than expected.